Dynamic interaction of BcsD subunit in type I bacterial cellulose synthase

Tatsuya Kondo[1], Yui Nakamura[2], Shingo Nojima[2], Min Yao[2], Tomoya Imai[1]

[1] Research Institute for Sustainable Humanosphere (RISH), Kyoto University, Uji, Kyoto 611-0011, Japan.

[2] Faculty of Advanced Life Science, Hokkaido University, N10W Kita-Ku, Sapporo 060-0810, Japan.

For correspondence:

Tomoya Imai, imai.tomoya.4c@kyoto-u.ac.jp; Research Institute for Sustainable Humanosphere, Kyoto University, Uji, Kyoto 611-0011, Japan.

Min Yao, yao@castor.sci.hokudai.ac.jp; Faculty of Advanced Life Science, Hokkaido University, N10W Kita-Ku, Sapporo 060-0810, Japan.

Running title: Dynamic interaction of BcsD in type I bacterial cellulose synthase

Keywords: cellulose, cellulose synthase, membrane enzyme, protein complex, protein-protein interaction, polysaccharide synthesis

Abstract

Cellulose is a promising biological material for supporting sustainable human life. This natural polymer is synthesized by cellulose synthase, a protein complex in the cell membrane. Cellulose synthase in bacteria is a hetero-subunit complex, and its subunit organization varies widely depending on the species. In the type I bacterial cellulose synthase complex, the BcsD (bacterial cellulose synthase D) protein is believed to play an important role in producing cellulose with long slender fiber morphology and high crystallinity, given the phenotype of the *bcsD*-deficient mutant and the specific existence of the type I operon in bacterial species synthesizing crystalline cellulose microfibrils such as Acetobacter. In this study, we successfully established a heterogeneously expressed Bcs protein in Escherichia coli as an experimental model and conducted biochemical studies for the BcsD protein and the other three major subunits of bacterial cellulose synthase, BcsA, BcsB, and BcsC. It has been shown that the BcsD protein interacts with the functionally required minimal subunits of the BcsAB complex, as well as the BcsC protein. Furthermore, it was shown that BcsD interacts with the BcsAB complex in two modes: direct protein-protein interactions and indirect interactions through the product cellulose. The former and latter modes represent the basal and active states of the type I bacterial cellulose synthase, respectively. This dynamic behavior of the BcsD protein is important for the type I bacterial cellulose synthase complex to regulate the crystallization process of cellulose.

38 **Introduction**

39 Cellulose is a natural polymer, whose molecular structure is composed of a homopolymer of glucose with
40 a β1→4 linkage, which is very simple. However, cellulose molecules are insoluble in water, and the apparent
41 elementary structure of cellulose is an aggregation of many cellulose molecules in long crystalline fibers.
42 This structural feature of cellulose underlies its structure-sustaining property, which many cellulose-
43 producing organisms rely on.

44 This polymer assembly is produced by the enzyme "cellulose synthase." In many known cases, *in vivo*
45 cellulose synthase is a protein complex with several polypeptide subunits. The most important subunit in this
46 complex is glycosyltransferase, which is called CesA. The first structural biological study of the CesA protein
47 was reported in 2013 for cellulose synthase from the bacterium *Rhodobacter sphaeroides* (1,2), which has
48 stimulated many biochemical studies on cellulose synthase.

49 Given its simplicity, bacterial cellulose synthase (Bcs) has been a model in many studies on cellulose
50 synthase. Particularly, Bcs from bacteria belonging to the genus *Acetobacter*, some of which are currently
51 named *Gluconacetobacter* or *Komagataeibacter* (the genus name "*Acetobacter*" is used for these bacteria in
52 this study), have been used extensively in studies. Although it is now known that many other bacteria produce
53 cellulose, the function and structure of cellulose appears to vary with species (3). For example,
54 phosphoethanolamine cellulose has been reported in *Escherichia coli*, and this natural cellulose derivative is
55 important for interacting with the host organism (4).

56 Among cellulose-synthesizing bacteria, *Acetobacter*, which has a gene cluster or operon categorized as

57 type I (3), is characteristic of synthesizing highly crystalline cellulose microfibrils (5) as well as plant
58 cellulose, a major natural source of cellulose. Previous studies have reported that the Bcs-complex in
59 *Acetobacter* is composed of at least four subunits (6,7) – BcsA (bacterial CesA, catalytic subunit), BcsB
60 (auxiliary subunit having a carbohydrate-binding domain and flavodoxin domain), BcsC (secretion of a
61 glucan chain through the outer membrane), and BcsD (crystallization subunit). In addition, endoglucanase
62 CMCax (8,9) (glycoside hydrolase family 8 (GH8)), unknown function protein Ccp (8,10) (also named as
63 BcsH (3)), and β-glucosidase bglAx (GH3) (11) are considered to be functionally involved in the complex.
64 Given that the cooperation of these subunits produces highly crystalline cellulose microfibrils, the spatial
65 organization of these subunits in the cell is important for understanding the cellulose biosynthesis mechanism
66 as a protein function (12).

67 In these subunits, the BcsD protein is found specifically in bacterial species producing highly crystalline
68 cellulose microfibrils such as *Acetobacter* and *Asaia* (3,13,14), which possess a type I Bcs-operon (3). The
69 *bcsD*-deficient mutant of *Acetobacter* showed a reduction in cellulose production, as well as a lack of ability
70 to synthesize crystalline cellulose microfibrils (6,7,15). Sunagawa *et al.* also demonstrated that BcsD
71 interacts with Ccp (BcsH) in a pull-down assay (16). Given that the BcsD protein contains glucan chains
72 inside its octamer structure (15), it has been proposed that BcsD is functionally located downstream of the
73 BcsAB complex (the cellulose-polymerizing core of the Bcs-complex (1,6,17,18)) (19,20). Detailed
74 information on how these functional units work together is key to understanding the mechanism by which
75 cellulose synthase can bundle the synthesized glucan chains for spinning a long slender crystalline fiber at

76 room temperature in an aqueous environment.

77 In this study, we analyzed protein-protein interactions in the type I Bcs-complex using the recombinant
78 BcsABCD protein with the *E. coli* expression system and clarified the interaction of BcsD with BcsAB
79 complex as well as BcsC protein. One of the advantages of using recombinant proteins is that mutant proteins
80 are easily available (21). Owing to this advantage, this study sheds light on the interaction between BcsAB
81 and BcsD and demonstrates that there are two modes for this interaction: direct protein-protein interactions
82 and indirect interactions through the cellulose molecules. We hypothesized that such bimodal interactions
83 between BcsAB and BcsD proteins could be key to controlling cellulose synthesis dynamically *in vivo*.

84

85 ## Results

86 **Production of endogenous *bcsA* gene-deficient *E. coli***

87 The expression of the *Acetobacter* Bcs complex in *E. coli* cells might lead to contamination by endogenous
88 *E. coli* Bcs (22).We then attempted to delete *bcsA* in the *E. coli* host, which encodes the catalytic subunit of
89 Bcs. The deletion of the *bcsA* gene in *E. coli* BL21, a strain expressing the Bcs recombinant protein in this
90 study, was performed using the Red/ET recombination system (Gene Bridges GmdH, Germany), in which
91 the *bcsA* gene was replaced by the FRT-PGK-gb2-neo-FRT cassette with homology arms of the *bcsA*-flanking
92 region using homologous recombination (Fig. 1A). This genetically modified BL21 (BL21-GM) strain was
93 confirmed by colony direct polymerase chain reaction (PCR) to contain the neomycin-resistance gene
94 cassette (FRT-PGK-gb2-neo-FRT cassette) (Fig. 1B). When amplified with primer #2 (antibiotic gene

95 cassette-specific) and #3 (*E. coli*-specific), a band of approximately 1,500 bp was found in BL21-GM, while
96 no specific product band was found in wild-type BL21, indicating the insertion of the neomycin-resistance
97 gene cassette specifically in BL21-GM. However, when amplified with primers #1 and #3 (either *E. coli*-
98 specific), wild-type BL21 and BL21-GM produced a band corresponding to the *bcsA* gene (2,818 bp) and
99 the inserted gene cassette (1,731 bp), respectively. These results confirmed the successful deletion of the
100 *bcsA* gene of BL21 in "BL21-GM."

101 Next, we measured the *in vivo* cellulose synthesis activity of the prepared BL21-GM (Fig. 1C) by partially
102 using our previous method (18): diguanylate cyclase (DGC) fused to thioredoxin ($_{Trx}$DGC) was expressed in
103 BL21 and BL21-GM to synthesize c-di-GMP to activate endogeneous bacterial cellulose synthase. The
104 amounts of cellulose synthesized were approximately 2.3 and 0.7 μg/mL of culture in BL21 and BL21-GM,
105 respectively. Although weak cellulose-synthesizing activity was observed, we used BL21-GM as a suitable
106 host to express the Bcs subunits with minimal impact on the endogenous Bcs-complex of *E. coli*.

107

108 **Characterization of BsCel5A**

109 Cellulase is an important tool used in this study to scrutinize the role of cellulose molecules in the subunit-
110 subunit interaction of the Bcs-complex. In this study, we used a bacterial endo-β-1,4-glucanase from *Bacillus*
111 *subtilis* (BsCel5A), whose structure has been previously reported (23). The full length (FL) of this cellulase
112 is a two-domain protein, in which the catalytic domain of GH5 is linked to the carbohydrate binding module
113 of family 3 (CBM3). In this study, the catalytic domain alone (CD) was also used to maximize access to the

114 soluble substrate. FL and CD of BsCel5A were expressed as glutathione-*S*-transferase (GST)-fused proteins
115 and purified with glutathione affinity resin, as confirmed by SDS-PAGE (Fig. S1A, left panel); (Fig. S1A,
116 left panel, white arrow). Activity-deficient mutant of E169Q/E257Q in FL (BsCel5A_FLm) and CD
117 (BsCel5A_CDm) was also used for a negative control protein in the cellulase treatment experiment.
118 The binding activity of the purified BsCel5A to phosphoric acid-swollen cellulose (PASC) was surveyed
119 to confirm correct folding of the expressed proteins. The results showed that all the BsCel5A proteins used
120 in this study retained their binding activity to PASC (Fig. S1A, right panel), indicating that all of them were
121 properly folded despite sequence modification. The enzymatic activity of BsCel5A was surveyed to
122 determine whether this cellulase could function at low temperature and neutral pH, which is required for
123 analyzing the Bcs-complex. Both BsCel5A_FL and BsCel5A_CD hydrolyzed barley β-glucan, carboxyl
124 methyl cellulose (CMC), and PASC at 4°C and pH 7.5 (Fig. S1B). For Avicel, full-length BsCel5A showed
125 higher activity than the others, stressing the function of CBM to bind solid cellulose.
126 Substrate specificity of BsCel5A was investigated using cello-oligosaccharides with various degrees of
127 polymerization (DP). BsCel5A hydrolyzed cellotetraose, cellopentaose, and cellohexaose but not cellobiose
128 or cellotriose (Fig. S1C). The final reaction products of BsCel5A for substrates longer than triose were
129 cellobiose and cellotriose, and the smallest substrate was cellotetraose (Fig. S1D).
130 Summarizing these, both BsCel5A_FL and BsCel5A_CD were able to hydrolyze cellulose of low
131 crystallinity at 4°C and pH 7.5, and cellulose molecules with DP higher than 3 were the substrates. This
132 information was considered when interpreting the data.

133

134 ***In vivo* cellulose synthase activity of recombinant Bcs-complex**

135 This study analyzed heterogeneously expressed Bcs proteins in *E. coli* as an experimental model. We then
136 checked if these heterogeneously expressed proteins were functional by using CESEC (cellulose-
137 synthesizing *E. coli*), a platform for estimating the cellulose-synthesizing activity with the co-expression of
138 diguanylate cyclase (DGC) (18). All the Bcs-complexes expressed in DGC-expressing BL21-GM
139 synthesized a significant amount of cellulose (Fig. 2A), indicating that each of the Bcs-complexes expressed
140 in this study are functional, regardless of whether BcsD is tagged. In addition, neither BcsAB nor the
141 BcsABCD complex with the activity-deficient mutant of the catalytic subunit BcsA (D333N or W373A)
142 showed cellulose-synthesizing activity, consistent with our previous study (21). These results support the
143 idea that the Bcs proteins expressed in this study reflect the state in function and are suitable for an
144 experimental model.

145 Despite the lower cellulose production shown in Fig. 2A, we decided to express Bcs proteins without co-
146 expression of DGC for subsequent purification because higher expression levels of Bcs proteins were
147 detected by western blotting (WB), as shown in Fig. 2B. Given that the cellulose quantification in this study
148 used strong acid treatment with acetic acid and nitric acid, we think that highly crystalline cellulose was
149 majorly considered in the data presented in Fig. 2A. Then it cannot be ruled out that the Bcs-complex
150 expressed in *E. coli* without DGC expression synthesizes cellulose.

151

152 **The complex formation of BcsAB, BcsC, and BcsD**

153 Given that BcsD holds the glucan chains in its channel (15), it is functionally located downstream of the
154 BcsAB complex, the core of cellulose molecule synthesis, indicating that BcsD operates in the periplasmic
155 space to assemble cellulose molecules extruded from the BcsAB complex. Furthermore, the BcsC protein
156 has a β-barrel porin-like structure at its C-terminus and is supposed to secrete cellulose through the outer
157 membrane (24). The results from several studies suggest that BcsAB, BscC, and BcsD work together in a
158 coordinated manner to spin bacterial cellulose. We tried to co-express BcsABCD to purify the whole Bcs-
159 complex using a hexa-histidine tag attached to the C-terminus of BcsD ($BcsD_{H6}$), as the tag at the C-terminus
160 does not disturb cellulose-synthesizing activity (16). After the optimization of the conditions (Fig. S2), all
161 four subunits were successfully purified together by immobilized metal affinity chromatography (IMAC)
162 (Fig. 3). This is the first successful purification of the BcsABCD complex ever reported. However, BcsC was
163 found to be mostly insoluble in detergent (*n*-dodecyl-β-D-maltoside, DDM, in this study) and tended to
164 degrade or aggregate during the purification process (Fig. 3A, BcsC antibody strip). We did not decipher
165 BcsC behavior in this Bcs-complex purification experiment.

166

167 **Analysis of the interaction between BcsAB and BcsD by cellulase treatment**

168 As described above, co-expression of $BcsABCD_{H6}$ in *E. coli* allowed the BcsABD-complex to be purified.
169 Given that $BcsABCD_{H6}$ expressed in *E. coli* is functional as shown in Fig. 2A, we speculated that a glucan
170 chain may link BcsAB and BcsD during this purification. This hypothesis was tested by checking whether

171 the digestion of cellulose resulted in the dissociation of BcsAB from $BcsD_{H6}$ during IMAC purification.
172 BsCel5A cellulase was applied to $BcsABCD_{H6}$ bound to IMAC resin prior to washing and elution. The
173 amounts of BcsA, BcsB, and BcsD proteins in the eluate were measured by semi-quantitative WB (Fig. 4A);
174 the reliability of quantification in our WB was confirmed, as shown in Fig. S3. The signal intensities of BcsA
175 and BcsB were normalized to that of BcsD in the eluate for comparison between samples. Notably, the
176 amounts of BcsA and BcsB bound to BcsD were decreased by BsCel5A treatment (Fig. 4B), indicating that
177 the BcsAB complex was detached from BcsD by cellulose digestion. This trend was clearer when
178 BsCel5A_CD was used as cellulase.

179 To rule out the possibility that the observed detachment of BcsAB was due to non-specific interaction of
180 the added BsCel5A protein, the activity-deficient mutant of BsCel5A (E169Q/E257Q) was applied to
181 $BcsABCD_{H6}$ bound to the metal affinity resin (Fig. 4, C and D). As a result of purification, no decrease in
182 the signal intensity of BcsA and BcsB was observed in the eluate, indicating that cellulose hydrolysis actually
183 caused detachment of BcsAB from BcsD during purification. In summary, the BcsAB complex indirectly
184 interacts with BcsD through the glucan chain.

185 Although cellulase treatment allowed the BcsAB complex to be detached from BcsD during purification,
186 as demonstrated above, a substantial portion of the BcsA and BcsB proteins remained with BcsD in this
187 purification process (Fig. 4B). We supposed that a direct interaction between BcsAB and BcsD is also found
188 in addition to the indirect interaction. To test this hypothesis, we attempted to purify the activity-deficient
189 mutants of $BcsABCD_{H6}$, $BcsA^{D333N}BCD_{H6}$, and $BcsA^{W373A}BCD_{H6}$, neither of which synthesize cellulose, as

190 shown in Fig. 2A. As a result, these mutants allowed BcsA and BcsB to be purified together with BcsD and
191 the wild type (Fig. 5A and B). Notably, cellulase treatment did not reduce the amount of BcsAB purified
192 together with BcsD for either $BcsA^{D333N}BCD_{H6}$ or $BcsA^{W373A}BCD_{H6}$ (Fig. 5C, 5D, and 5E). These results
193 support the existence of a direct interaction between BcsAB and BcsD when cellulose is not synthesized.
194 Compiling these cellulase treatment experiments, it was demonstrated that there are two modes of interaction
195 between BcsAB and BcsD: direct and indirect modes through cellulose molecules.
196
197 **Quaternary structure of the Bcs-complex**
198 Despite the demonstration of two modes for the interaction between BcsAB and BcsD, the quaternary
199 structure of the entire Bcs-complex remains to be elucidated. We then performed pull-down assays to further
200 explore the subunit-subunit interactions in the BcsABCD complex by fully utilizing recombinant Bcs
201 proteins. The assay was designed based on the results from previous studies (Fig. 6A): (i) BcsAB forms a
202 complex in the inner membrane (1), (ii) BcsC is an outer membrane protein (24,25), (iii) BcsD protein is
203 located in the periplasmic space (15,20), and (iv) BcsD interacts with the BcsAB complex (this study).
204 First, the interaction between BcsAB and BcsD, which has been demonstrated above, was tested by pull-
205 down with a bait of Streptag(II)-fused BcsD ($BcsD_{StrepII}$) and a prey of crude BcsAB without tags (DDM-
206 solubilized cell membrane of *E. coli* expressing BcsAB). As expected, BcsAB bound to $BcsD_{StrepII}$ (Fig. 6B).
207 The pull-down assay yielded a result consistent with our purification experiment of the BcsABD-complex
208 and supported our hypothesis for the interaction between BcsAB and BcsD.

209 Given the successful pull-down assay with BcsAB and $BcsD_{StrepII}$, we next performed a pull-down assay
210 to survey the BcsC-involved interaction in the complex (see Fig. 6A). For this purpose, TPR tetratricopeptide-
211 repeat (TPR) domain of the BcsC protein (BcsC_TPR) was used based on two assumptions: (i) the role of
212 the TPR domain is protein-protein interaction (26), and (ii) the full-length BcsC protein is unstable, as shown
213 in our purification. Pull-down by $BcsD_{StrepII}$ trapped $_{H6}BcsC_TPR_{H6}$, which has hexa-histidine tags at both
214 the N- and C-termini of BcsC_TPR, in a dose-dependent manner (Fig. 6C), clearly showing that these two
215 proteins interact with each other. Furthermore, pull-down by the purified $_{H6}BcsC_TPR_{H6}$ (bait) with the crude
216 BcsAB (prey) also supported their interaction with each other (Fig. 6D), although it appeared less striking
217 than the case with $_{H6}BcsC_TPR_{H6}$ and $BcsD_{StrepII}$ (Fig. 6C).
218 Finally, we performed a pull-down assay using all subunits in the complex: crude BcsAB, purified
219 $_{H6}BcsC_TPR_{H6}$, and purified $BcsD_{StrepII}$ (Fig. 6E). Streptactin beads trapped BcsA, BcsB, and $_{H6}BcsC_TPR_{H6}$
220 together with $BcsD_{StrepII}$, although BcsA was only faintly detected by WB. It is then summarized that the
221 BcsD protein can simultaneously interact with BcsA, BcsB, and the TPR region of BcsC.
222

223 **Discussion**

224 Bacterial cellulose synthase is a heterosubunit complex. Primary evidence for this hypothesis is the
225 existence of gene clusters or operons encoding cellulose synthase-related genes (3,6,7,11). However, this
226 hypothetical model has not been tested intensively, owing to the lack of studies on the protein. Two recent
227 reports have addressed this question. Sunagawa et al. demonstrated an interaction between BcsD and BcsH

228 (Ccp) proteins using a pull-down assay (16). Another prominent study was the X-ray crystallographic
229 analysis of the BcsAB protein complex by Morgan et al., which clarified that the BcsA and BcsB proteins
230 closely interact with each other to polymerize and translocate the glucan chain from the cytosol to the
231 extracellular side (1), as confirmed also in *E.coli* (27). In this study, we analyzed the type I Bcs complex and
232 demonstrated that the BcsD protein interacted with the BcsAB complex (Fig. 3, 4, 5, and Fig. 6B) and the
233 TPR domain of BcsC (Fig. 6C). Furthermore, it was shown that BcsC_TPR interacted with the BcsAB
234 complex, although the result was not as clear as the interaction between BcsC_TPR and BcsD (Fig. 6D).
235 Finally, a pull-down assay using $BcsD_{StrepII}$ with a mixture of crude BcsAB and purified $_{H6}$BcsC_TPR $_{H6}$
236 indicated that BcsD binds to both BcsAB and BcsC_TPR simultaneously, suggesting that these four subunits
237 interact with each other (Fig. 6E). Our study, together with previous studies, experimentally demonstrated
238 that the subunits of BcsA, BcsB, BcsC, BcsD, and BcsH are included in the type I Bcs-complex.

239 Interestingly, this study showed that the interaction of BcsD with BcsAB has two modes: direct and indirect
240 interactions through the polymerized glucan chain (Fig. 4). Direct interaction between the BcsAB complex
241 and BcsD protein was observed for both wild type and catalytically deficient mutant cellulose synthase,
242 whereas the interaction via cellulose was observed only for the wild type (Fig. 5). We then propose a two-
243 state model for the type I Bcs complex: basal and active states, which are represented by the direct interaction
244 (Fig. 7, left) and indirect interaction modes (Fig. 7, right), respectively.

245 BcsD protein in this basal state is statically fixed on the BcsAB complex for lying in wait for a glucan
246 chain synthesized by the BcsAB complex. Once cellulose synthesis is initiated, the synthesized glucan chain

247 is guided into the octameric ring of BcsD to crystallize cellulose molecules, as proposed previously
248 (7,15,16,20,28), which is a shift from the resting state to the active state of the complex. In the active state
249 (Fig. 7, right), the BcsD protein is detached from the BcsAB complex but tethered to BcsAB by the glucan
250 chain extruded from BcsAB. Considering the substrate specificity of BsCel5A (Fig. S1), BcsD can be
251 physically separated from BcsB by a glucan chain with a length of four or more glucose residues (Fig. 7).

252 In this two-state model, the active state of the Bcs complex allows BcsD to be launched toward the outer
253 membrane, while BcsD in the basal state may be fixed statically on BcsB. The TPR domain of the BcsC
254 protein may control diffusible BcsD in the active state in the periplasmic space by gentle but significant
255 interactions. Given that the C-terminal domain of BcsC is an outer membrane β-barrel channel (Fig. S4) (24),
256 the TPR domain of BcsC may escort BcsD carrying glucan chains toward the outer membrane channel in
257 BcsC to spin the glucan chains to the extracellular side. The following questions about this model will be
258 whether (i) BcsD protein could dock to the outer membrane channel part of the BcsC protein and (ii) the
259 interaction between BcsC and BcsD could be state-dependent. These questions will be addressed in future
260 studies to enhance our understanding of the Bcs-complex function.

261 Our study demonstrated the intermolecular interactions of subunits in the BcsABCD complex to update
262 our knowledge of the quaternary structure of the type I Bcs complex. Experiments in this study were
263 performed using recombinant proteins heterogeneously expressed in *E. coli*; thus, further studies will be
264 necessary to test the hypothesis proposed in this study, the two modes for BcsAB-BcsD interaction: the basal
265 and the active state. Nonetheless, the data obtained in this study were intensively tested using mutagenesis

266 experiments of proteins, and they were consistent with each other. We believe that our hypothesis in this
267 study is sufficiently reliable, at least for starting further discussion about the mechanism of Bcs with regard
268 to protein function. In this model, BcsD is not statically fixed in the Bcs-complex but dynamically interacts
269 with the other subunits in the complex (Fig. 7). Such a dynamic behavior may be involved in the
270 crystallization function of cellulose molecules, as well as twisting in bacterial cellulose microfibrils, as
271 reported previously (16). The putative state control with BcsD, as shown in Fig. 7, is the regulation of the
272 quaternary structure of bacterial cellulose synthase. Next, we need to further study the original *Acetobacter*
273 cells and observe the whole Bcs-complex at higher resolution with cryo-EM under controlled two-state
274 conditions.
275

276 **Experimental procedures**

277 **Chemicals**

278 All chemicals used in this study were purchased from FUJIFILM Wako Pure Chemicals Co. Ltd. (Osaka,
279 Japan), Nacalai Tesque Co. Ltd. (Kyoto, Japan), and Sigma-Aldrich Inc. (MO, USA), unless otherwise
280 indicated.
281

282 **Cloning**

283 Bcs genes (*bcsA*, *bcsB*, *bcsC*, and *bcsD*) were prepared from genomic DNA extracted from cultured cells
284 of *Komagataeibacter sucrofermentans* JCM9730, which was provided by the RIKEN Bio Resource Center

285 (Tsukuba, Japan) and known by the strain name BPR2001 (29,30). The endo-β1,4-glucanase gene from
286 *Bacillus subtilis* strain 168 (*bscel5A*) (23) was prepared from the genomic DNA provided by the American
287 Type Culture Collection (ATCC23857D). The dgc gene (*dgc*) was identical to that used in our previous study
288 (18): tDGC and DGC from *Thermotoga maritima* MSB8 with a point mutation of R158A and truncation of
289 the N-terminal 81 amino acid residues from V1 to V81 (31). The gene for green fluorescent protein UV
290 (GFPuv) (32) was prepared from the pGFPuv plasmid purchased from Takara Bio, Co. Ltd. (Shiga, Japan).
291 The cloning of these genes was performed by PCR using PrimeStarGXL (Takara Bio Co. Ltd.). Site-
292 directed mutagenesis was performed by QuikChange II (Agilent Inc., CA, USA) or the equivalent PCR-based
293 method. The sequence of the PCR-amplified DNA was checked by the dye-terminator method in a subcloning
294 vector (pGEM-T easy (Promega Inc., WI, USA) or pTAC-2 (BioDynamics Laboratory Co. Ltd., Tokyo,
295 Japan)), or final expression vector, which was performed at either of the Uji DNA-sequencing core (Kyoto
296 University Research Administration Office) with an ABI Prism 310 Genetic Analyzer (Applied Biosystems
297 Inc., MA, USA), or Eurofins Genomics Inc. (Tokyo, Japan).
298
299 **Construction of the expression vectors**
300 The protein expression vectors used in this study are summarized in Table 1. Expression vectors for BcsAB
301 (BcsAB, $BcsA^{D333N}B$, and $BcsA^{W373A}B$) were identical to those used in previous studies (18,21). The *bcsAB*
302 gene in the operon form was inserted between the EcoRI and KpnI sites in pQE-80L (Qiagen, Hilden,
303 Germany), and the upstream of the start codon was the original ribosomal binding site of *K. sucrofermentans*

304 JCM9730.

305 Expression vectors for BcsABCD (BcsABCD, $BcsABC_{H6}D$, $BcsABCD_{H6}$, $BcsA^{D333N}BCD_{H6}$,

306 $BcsA^{W373A}BCD_{H6}$, and $BcsABCD_{GFPuvH6}$) proteins were constructed from the vectors for BcsAB by inserting

307 the *bcsABCD* gene in the operon form between the EcoRI and HindIII sites in pQE-80L. The ribosomal

308 binding site in these BcsABCD expression vectors is exactly the same as that in the expression vectors of

309 BcsAB, one of *K. sucrofermentans* JCM9730. DNA encoding the tag (hexa-histidine or GFPuv) was added

310 to *bcsD* during the PCR-amplification amplification.

311 The expression vectors for the TPR region of BcsC (BcsC_TPR: C18-G848) and BcsD were prepared for

312 the pull-down assay. DNA encoding hexa-histidine tag was added to the 3′-end of the gene for BcsC_TPR

313 during PCR amplification and inserted into the NdeI and XhoI sites in pET-28b (Merck Corp.., Darmstadt,

314 Germany) to express BcsC_TPR protein with dual hexa-histidine tag at both N- and C- terminal –

315 $_{H6}BcsC_TPR_{H6}$. DNA encoding Streptag (II) was added to the 3′-end of the gene for BcsD and inserted

316 between the NcoI and HindIII sites in pET28b to express BcsD with C-terminal Streptag(II)–$BcsD_{StrepII}$.

317 The gene for tDGC was inserted between the NdeI and HindIII sites in pBAD33et32, a customized plasmid

318 DNA in this study, to express the thioredoxin-fused tDGC protein to count the cellulose-synthesizing activity

319 of the recombinant BcsAB and BcsABCD complex in our previous studies (18,21). The detailed procedure

320 for preparing pBAD33et32 is described in Supplementary Information. Thioredoxin gene (*trx*) in

321 pBAD33et32 was copied from pET32a (Merck Corp.) to replace the His-patch thioredoxin used in our

322 previous study (18), which was derived from pBAD202-TOPO (Invitrogen Inc., MA, USA).

323 For the bacterial endoglucanase gene *bscel5A*, the putative signal peptide sequence (M1–A28) was
324 removed from the full-length construct. Full-length (A29–N499) and catalytic domain (A29–T332) genes
325 were inserted between BamHI and XhoI sites in pGEX4T-3 (Cytiva Inc., MA, USA) to express the N-
326 terminal GST-fused endoglucanase BsCel5A.
327
328 **Deletion of *bcsA* gene from *Escherichia coli* BL21**
329 In this study, we used genetically modified *E. coli* BL21 to express Bcs proteins, which lack the whole
330 *bcsA* gene (Fig. 1A). This gene manipulation was performed using the Red/ET recombination system (Gene
331 Bridges GmbH, Heidelberg, Germany), according to the manufacturer's specifications. The detailed
332 procedure is described in Supplementary Information.
333 Briefly, *E. coli* BL21 strain (purchased from New England Labs Inc., MA, USA) was transformed with
334 the pRedET plasmid carrying the genes for DNA-recombination proteins and selected by tetracycline
335 resistance. The second transformation was followed by introducing linear DNA of neomycin-resistant gene
336 flanked by the homology arm sequences corresponding to the upstream and downstream of *bcsA* gene
337 (CP010816.1); the recombinant proteins were expressed with arabinose-induction for disrupting *bcsA* gene,
338 and subsequently the pRedET plasmid was expelled out of the cell by culturing at 37°C. Finally, the *bcsA-*
339 *disrupted* BL21 transformant was selected for kanamycin resistance and tetracycline sensitivity. Gene
340 modification was confirmed by direct PCR (Fig. 1B). We named this genetically modified *E. coli* BL21 strain
341 as BL21-GM. Chemically competent cells of BL21-GM were then prepared by treating the cultured cells in

342 a rubidium-based buffer according to the protocol on the website of the Center for Molecular Biology and
343 Genetics at Mie University (https://www.gene.mie-u.ac.jp/Protocol/Original/Transform-Comp-Cell-
344 Freeze.html, in Japanese) (33).
345
346 ***In vivo* cellulose synthase activity**
347 The endogenous cellulose-synthesizing activity of *E. coli* and cellulose-synthesizing activity of the
348 heterogeneously expressed Bcs-complex in *E. coli* was estimated by expressing DGC protein to activate
349 bacterial cellulose synthase in the cell by the produced c-di-GMP (18). In this study, the pBAD33et32-tDGC
350 plasmid was used to express the DGC. The obtained *E. coli* transformants were pre-cultured in LB medium
351 including the proper antibiotics at 37°C overnight, and then 0.1 mL of the pre-culture was inoculated into 10
352 mL of ZYP-5052 medium with 50 μg/mL chloramphenicol (100 μg/mL ampicillin when expressing Bcs-
353 complex) and 0.001% L-arabinose. Cells were grown at 20°C in an orbital shaker at 180 rpm for 24 h and the
354 cultured cells were collected by centrifugation at 2,000 × *g* for 20 min. The amount of cellulose in the pellet
355 was quantified using the anthrone-sulfuric acid method (34) as described below.
356 Two milliliters of AN-reagent (a mixture of glacial acetic acid and nitric acid with volumetric ratio of 8:1)
357 were added to the pellet and then heated at 105°C for 30 min. The remaining cellulose pellets were washed
358 with 10 mL of water once by centrifugation at 2,000 × *g* for 10 min, and then 1 mL of 72% (v/v) H_2SO_4 was
359 added to the pellets and incubated for 1 h at room temperature. The solution (0.1 mL) was mixed with water
360 (0.4 mL), and then, 1 mL of fresh anthrone reagent (0.2% w/v anthrone in concentrated H_2SO_4) was added

361 and mixed. The solution was heated to 90°C for 15 min and allowed to stand until it reached room temperature

362 (approximately 15 min). The absorbance of the solution was measured at both 625 and 700 nm, and the

363 absorbance at 625 nm, from which the absorbance at 700 nm was subtracted, was used for quantification for

364 better reproducibility. Calibration was performed with phosphoric acid-swollen cellulose (PASC) prepared

365 using a previously reported protocol (35).

366

367 **Purification and characterization of BsCel5A**

368 Expression of GST-fused BsCel5A endoglucanase was performed in *E. coli* BL21 (not GM strain): all the

369 four constructs ((BsCel5A_FL, BsCel5A_CD, BsCel5A_FL^{m}, and BsCel5A_CD^{m}) were expressed and

370 purified in the same manner.

371 The transformant of BL21 with pGEX-BsCel5A were inoculated in 10 mL LB containing 100 μg/mL

372 ampicillin in a 100 mL flask and grown at 37°C with orbital shaking at 220 rpm overnight. The cells were

373 harvested by centrifugation at 3,000 × *g* for 20 min, suspended in 1 L of LB containing 100 μg/mL ampicillin

374 in a 5 L baffle flask, and cultured at 37°C until OD_{600} reached 0.6. The culture medium was cooled in ice

375 water for 10 min, and then IPTG was added to 0.1 mM and incubated at 20°C for 20 h at 160 rpm with

376 shaking.

377 The cells were then collected at 3,000 × *g* for 20 min, washed with 40 mL of 1 × phosphate-buffered saline

378 (PBS), suspended in 40 mL of 1 × PBS containing 1 mM phenylmethylsulfonyl fluoride (PMSF), and

379 sonicated on ice for ~5 min (exposure: 10 s, rest: 50 s; until slightly translucent). The cell lysate clarified by

380 20,000 × *g* for 30 min at 2°C was applied to 5 mL of Glutathione Sepharose 4B (Cytiva Inc,), washed with
381 20 mL of 1 × PBS, and eluted with 5 c.v. of 0.1 M Tris-HCl pH 8.0, 0.5 M NaCl, 20 mM reduced-glutathione.
382 The eluted fraction was buffer exchanged with 1 × PBS using Vivaspin 6 (MWCO 10 kDa; Sartorius AG,
383 Germany).

384 To remove the GST tag fused to the N-terminus, 100 units of thrombin (Merck Corp.) was added to 10 mg
385 of $_{GST}$BsCel5A and incubated at 20°C for two days. Thrombin was then removed by adding 1 mL of
386 Benzamidine Sepharose 6 B (Cytiva Inc.), and the cleaved GST was removed by adding 5 mL of Glutathione
387 Sepharose 4 B. A solution of PMSF was added to the obtained BsCel5A protein at a final concentration of 1
388 mM to inactivate a small amount of residual thrombin.

389 The recombinant BsCel5A proteins purified were characterized with regard to the following points: (i)
390 binding activity to cellulose, (ii) glycoside hydrolase activity, and (iii) substrate specificity. The detailed
391 experimental procedure is described in Supplementary Information.

392

393 **Purification of BcsABCD complex**

394 All the protein purification experiments in this study were performed at low temperature (~4°C). The
395 composition of the protease inhibitor mix (PI) used for protein purification was as follows: 0.1 mM PMSF, 1
396 mM benzamidine-HCl, 5 μM bestatin, 10 μM leupeptin, 1 μM pepstatin A.

397 The transformant of *E. coli* BL21-GM with pQE-BcsABCD$_{H6}$ was inoculated in 10 mL of LB containing
398 100 μg/mL ampicillin in a 100 mL flask and grown at 37°C with shaking at 220 rpm overnight. The cells

399 were harvested by centrifugation at 3,000 × *g* for 20 min, resuspended in 1 L of ZYP-5052 containing 100

400 μg/mL ampicillin and 0.0005% (v/v) antifoam SI (Fujifim Wako Chemicals Co. Ltd., Japan) in a 5 L baffle

401 flask, and incubated at 20°C for 22 h with an orbital shaker at 100 rpm. The cultured cells were collected at

402 3,000 × *g* for 20 min and suspended in 50 mL of buffer A (20 mM sodium phosphate buffer (pH 7.5), 300

403 mM NaCl, 8% glycerol, 5 mM $MgCl_2$, 5 mM cellobiose) with PI, prior to cell lysis by two passes of high-

404 pressure homogenizer (French Press, Thermo Fisher Scientific Inc., MA, USA) at a pressure of 15,000 psi.

405 The lysate clarified by centrifugation at 5,000 × *g* for 10 min and ultracentrifugation at 150,000 × *g* for 30

406 min at 2°C. The obtained cell membranes were resuspended in buffer A with PI and NaCl concentrations

407 increased to 1 M and were ultracentrifuged again under the same conditions. Finally, the cell membrane was

408 suspended in buffer A with PI to approximately 10 mg/mL (estimated by the DC protein assay, Bio-Rad Inc.,

409 CA, USA). The collected cell membrane was stored at -80°C until use in experiments.

410 Ten milliliters of the cell membrane suspension were mixed with *n*-dodecyl-β-D-maltopyranoside (DDM)

411 at a final concentration of 0.5% (w/v) and shaken gently for 1 h at 4°C for solubilizing Bcs-complex.

412 Supernatant of the following ultracentrifugation at 150,000 × *g* for 30 min at 2°C was collected as solubilized

413 fraction, and imidazole stock solution (2 M, pH 8.0) was added to achieve a final concentration of 10 mM,

414 prior to loading to 0.4 mL a His-Select Cobalt Affinity Gel (Sigma-Aldrich Inc.), which was equilibrated

415 with 4 mL of wash buffer (20 mM imidazole and 0.025% (w/v) DDM in buffer A) in advance. After loading

416 the solubilized protein onto the affinity resin in a plastic open column, the resin in the column was washed

417 with 3 mL of wash buffer and finally eluted with elution buffer (200 mM imidazole and 0.025% (w/v) DDM

418 in buffer A).

419

420 **Cellulase treatment of Bcs-complex**

421 Cellulase treatment of $BcsABCD_{H6}$ was performed using a cobalt affinity gel. The same procedure was
422 followed for the binding step of $BcsABCD_{H6}$ on the affinity gel. After all the solubilized fraction passed
423 through the column, 0.8 mL of 1.5 μM BsCel5A solution in wash buffer (20 mM imidazole and 0.025% (w/v)
424 DDM in buffer A) was loaded to the column. The column exit was plugged when most of the cellulase
425 solution passed, and then the gel was incubated at 10°C for 3 h with the remaining cellulase solution. After
426 unplugging, the affinity gel in the column was washed with 2 mL of wash buffer and eluted with elution
427 buffer (200 mM imidazole and 0.025% (w/v) DDM in buffer A).

428

429 **Protein preparation for pull-down assay: BcsC_TPR, BcsD, and crude BcsAB**

430 The pull-down assay in this study used purified BcsC_TPR, purified BcsD, and crude BcsAB proteins,
431 each of which was prepared as described below.

432 The transformant of *E. coli* BL21(DE3) with pET-$_{H6}$BcsC_TPR$_{H6}$ was inoculated in 10 mL of LB
433 containing 50 μg/mL kanamycin in a 100 mL flask and grown at 37°C with shaking at 220 rpm overnight.
434 The cells were harvested by centrifugation at 3,000 × *g* for 20 min, and resuspended in 1 L of ZYP-5052 (36)
435 containing 200 μg/mL kanamycin and 0.0005%(v/v) antifoam SI in a 5 L baffle flask, and incubated at 20°C
436 for 24 h in a shaking incubator at 100 rpm. The cultured cells were collected at 3,000 × *g* for 20 min, and

437 washed with 40 mL of 1 × PBS prior to resuspension in 100 mL of 10 mM imidazole in buffer B (20 mM
438 sodium phosphate buffer (pH 7.5), 500 mM NaCl, 8% glycerol) with PI, and sonicated on ice for ~5 min
439 (exposure: 10 s, rest: 50 s; until slightly translucent). The cell lysate was clarified by centrifugation at 40,000
440 × *g* for 30 min at 2°C and applied to 4 mL a His-Select Cobalt Affinity Gel (Sigma-Aldrich Inc.), followed
441 by washing with 10 mM imidazole in buffer B, and eluted 250 mM imidazole in buffer B. Finally, the buffer
442 of eluted fraction including $_{H6}$BcsC_TPR$_{H6}$ protein was replaced with buffer B using PD-10 desalting column
443 (Cytiva Inc.).

444 The BcsD protein was expressed in *E. coli* BL21(DE3) with pET-BcsD$_{StrepII}$. The transformant was
445 inoculated in 10 mL of LB containing 50 μg/mL kanamycin in a 100 mL flask and grown at 37°C with
446 shaking at 220 rpm overnight. The cells were harvested by centrifugation at 3,000 × *g*, 20 min, resuspended
447 in 1 L of LB containing 50 μg/mL kanamycin in a 5 L baffle flask and cultured at 37°C until OD_{600} was ~0.6.
448 The culture medium was cooled in ice water for 30 min, and IPTG (0.5 mM) was added and incubated at
449 25°C for 20 h at 120 rpm. Cells were collected at 3,000 × *g* for 20 min, suspended in 30 mL of buffer C (20
450 mM Tris-HCl (pH 7.5), 150 mM NaCl, and 1 mM EDTA) with PI, and sonicated on ice for ~10 min
451 (exposure: 10 s, rest: 50 s; until slightly translucent). The cell lysate was centrifuged at 20,000 × *g* for 30 min
452 at 2°C, applied to 2 mL of Streptactin Sepharose HP (Cytiva Inc.), washed with 20 mL of buffer C, and eluted
453 with 4 mM *d*-desthiobiotin in buffer C. Finally, buffer of eluted fraction was replaced by buffer C using
454 Amicon Ultra-4 MWCO 50 kDa (Merck Corp.).

455 The crude protein of BcsAB was prepared using the transformant *E. coli* BL21-GM with pQE carrying the

456 *bcsAB* gene. The procedure to isolate the cell membrane, from culture to ultracentrifugation, was same as in

457 the case of $BcsABCD_{H6}$ as described previously, except for the buffer to suspend the cells and cell membrane:

458 buffer D (20 mM sodium phosphate buffer (pH 7.5), 100 mM NaCl, 8% glycerol, 5 mM $MgCl_2$, and 5 mM

459 cellobiose) with PI was used. The obtained cell membrane was suspended in buffer D with PI at

460 approximately 10 mg/mL (estimated by the DC protein assay, Bio-Rad Inc.). Finally, crude BcsAB protein

461 was prepared by solubilizing 7 mL of the cell membrane fraction with 0.5% (w/v) DDM for 1 h and

462 centrifugation at 150,000 ×*g* for 30 min at 2°C.

463

464 **Pull-down assays**

465 For the pull-down by $BcsD_{StrepII}$ with the crude BcsAB, purified $BcsD_{StrepII}$ (0.2 mg) was added to 7 mL of

466 crude BcsAB, incubated for 3 h at 4 °C, and then loaded to 0.1 mL of Streptactin Sepharose HP. The resin

467 was washed with 1 mL of 0.025% (w/v) DDM in buffer D, and finally the bound protein was eluted with 4

468 mM desthiobiotin in buffer D with 0.025% (w/v) DDM.

469 For the pull-down assay, $BcsD_{StrepII}$ with $_{H6}BcsC_TPR_{H6}$, $BcsD_{StrepII}$ (0.1 mg) were incubated with

470 $_{H6}BcsC_TPR_{H6}$ (0, 0.1, 0.3, 0.5 mg) in 3 mL of buffer D (–/–) (buffer D without $MgCl_2$ and cellobiose) for 3

471 h at 4 °C, and then loaded to 0.1 mL of Streptactin sepharose HP. After washing with buffer D (–/–), the

472 bound protein was eluted with 1 mL 4 mM *d*-desthiobiotin in buffer D (–/–).

473 For the pull-down assay by $_{H6}BcsC_TPR_{H6}$ with BcsAB, purified $_{H6}BcsC_TPR_{H6}$ (0.2 mg) was mixed with

474 crude BcsAB (7 mL), and further NaCl stock solution was added to set 500 mM NaCl in the final solution.

475 After incubation for 1 h at 4 °C, the sample was loaded to 0.2 mL a His-Select Cobalt Affinity Gel and washed
476 with 2 mL of 20 mM imidazole in buffer B (+/+) (buffer B with 5 mM $MgCl_2$ and 5 mM cellobiose) with
477 0.025% (w/v) DDM. The bound protein was eluted with 200 mM imidazole in buffer B containing 0.025%
478 (w/v) DDM.

479 Finally, we performed a pull-down assay using $BcsD_{StrepII}$, purified BcsC_TPR; crude BcsAB. $BcsD_{StrepII}$
480 (0.2 mg) and $_{H6}BcsC_TPR_{H6}$ (0.2 mg) were mixed with crude BcsAB (7 mL of DDM extract); NaCl stock
481 solution (5 M) was added to a final concentration of 500 mM NaCl. After incubation for 3 h at 4 °C, the
482 sample solution was loaded to 0.1 mL of Streptactin Sepharose HP. After washing with 1 mL of buffer B
483 (+/+) containing 0.025% (w/v) DDM, the bound protein was eluted with 4 mM *d*-desthiobiotin in buffer B
484 (+/+) containing 0.025% (w/v) DDM.

485 Prey protein without bait protein was used as a negative control for the pull-down assay using the same
486 procedures. The eluted fraction was analyzed by SDS-PAGE, followed by WB as described later.

487

488 **Western blotting (WB) analysis**

489 Rabbit polyclonal antibodies against BcsA, BcsB, BcsC, and BcsD proteins were generated with the
490 synthetic peptide corresponding to a part of the C-terminus of BcsA (18,20,21,37), the C-terminus of BcsB
491 (this study), the C-terminus of BcsC (37), and the loop between the β3 and β4-strand (20,37). The dilution
492 rate was 10,000-fold for anti-BcsA, anti-BcsB, and anti-BcsC, whereas anti-BcsD was diluted 20,000-fold.
493 Each of the antibodies against the peptide tag were diluted as follows: anti-Strep tag II (15 ng/mL; ab180957,

494 Abcam Corp., Cambridge, UK), anti-His5 (0.1 μg/mL; 34660, Qiagen N.V., Germany), and anti-Thioredoxin

495 (1 μg/mL; ab139677, Abcam Corp.).

496 Horseradish peroxidase (HRP)-conjugated anti-rabbit IgG (W401B; Promega Inc.) and HRP-conjugated

497 anti-mouse IgG (7076S; Cell Signaling Technology Inc., MA, USA) were diluted 20,000-fold and used as

498 the secondary antibodies. ECL-Prime (Cytiva Inc.) was used for chemical luminescence with HRP.

499 For the WB with anti-BcsD, anti-Strep, anti-His, and anti-thioredoxin, the samples for SDS-PAGE were

500 heat-treated at 100°C for 3 min after mixing with the sample buffer, while the samples to visualize by the

501 other antibodies were incubated in the sample buffer for several minutes at room temperature. The samples

502 were analyzed by SDS-PAGE with a precast polyacrylamide gel (SuperSep Ace 5-20%, Fujifim Wako

503 Chemicals Co. Ltd.), and blotting from the gel to PVDF membrane (Immobilon-P, 0.45 μm-ϕ, Cytiva Inc.)

504 was done by a constant current mode at 150 mA/10 cm^2 for 30 min. Blocking of the membrane was performed

505 with 0.3% skim milk and 0.02% NaN_3 in tris-buffered saline (TBS) containing 0.05% Tween-20 (TBS-T),

506 for the WB with anti-Bcs proteins, while blocking was performed with 2.5% BSA, 0.1% gelatin, 0.02%

507 Tween-20, 0.04% NaN_3 in PBS at 4°C overnight or at room temperature for 0.5–1 h, for either of anti-Strep-

508 tag II, anti-His5, or anti-thioredoxin. The membranes were briefly rinsed with TBS-T and then subjected to

509 the primary antibody reaction in blocking buffer for 1–2 h at room temperature. After removing the antibody

510 solution, the membrane was briefly rinsed and washed with TBS-T thrice for 5 min, followed by a secondary

511 antibody reaction in TBS-T for 30–45 min at room temperature. The membrane was briefly rinsed and

512 washed with TBS-T three times for 15 min each time. The protein bands were then visualized by casting the

513 ECL prime solution on the blotted PVDF membrane (0.2 mL/9 cm^2 membrane), and digitally recorded with

514 AE-9300H EZ-Capture MG (ATTO Co. Ltd., Japan).

515 Quantitative analysis was performed using ImageJ (version 1.53a) to quantify the band signal intensity,

516 calculated as relative values to the negative control, and the relative signal intensities of BcsA and BcsB were

517 normalized to the signal intensity of BcsD. For BcsA; two major bands were reproducibly observed near the

518 75-kDa and 250-kDa marker (Fig. 2B, top row), as well as in our previous studies (18,37), which are probably

519 BcsA monomer and BcsA-including oligomer, respectively (the estimated molecular weight for the BcsA

520 monomer is 84 kDa). Given these observations, the band intensity for the BcsA-containing oligomer was

521 also considered in addition to the monomer band intensity in subsequent analyses.

522

523 **Data availability**

524 All data are contained within this article and available from the corresponding author on reasonable

525 request.

526

527 **Supporting information**

528 This article contains supporting information.

529

530 **Acknowledgments**

531 The authors thank Dr. Kenji Tajima of Hokkaido University for his advice. The authors thank Professor

Ryoichi Yamaji and Dr. Yasuyuki Kobayashi at Osaka Prefecture University for their advice regarding the pull-down assay.

Author contributions

T. I., and M. Y. conceptualization; T. K., T. I., and M. Y. methodology; T. K. formal analysis, T. K., N. Y., and S. N. investigation; T. I. resources; T. K., and T. I. data curation; T. K., and T. I. writing-original draft; T. K., M. Y., and T. I. writing-review and editing; T. K., and T. I. visualization; T. I., and M. Y. supervision; T. K., M. Y., and T. I. project administration; T. I. funding acquisition.

Funding and additional information

This work was supported by JPSP KAKENHI (grant numbers 15H04530 and 19H00950), Exploratory Research on Humanosphere Science (RISH, Kyoto University), and JST CREST (grant number: JPMJCR13B2).

Conflict of interest

The authors declare that they have no conflicts of interest with the contents of this article.

551 **References**

552 1. Morgan, J. L. W., Strumillo, J., and Zimmer, J. (2013) Crystallographic snapshot of cellulose
553 synthesis and membrane translocation. *Nature* **493**, 181-186

554 2. Morgan, J. L. W., McNamara, J. T., and Zimmer, J. (2014) Mechanism of activation of
555 bacterial cellulose synthase by cyclic di-GMP. *Nat. Struct. Mol. Biol.* **21**, 489-496

556 3. Römling, U., and Galperin, M. Y. (2015) Bacterial cellulose biosynthesis: Diversity of
557 operons, subunits, products, and functions. *Trends Microbiol.* **23**, 545-557

558 4. Thongsomboon, W., Serra, D. O., Possling, A., Hadjineophytou, C., Hengge, R., and Cegelski,
559 L. (2018) Phosphoethanolamine cellulose: A naturally produced chemically modified
560 cellulose. *Science* **359**, 334-338

561 5. Tajima, K., Imai, T., Yui, T., Yao, M., and Saxena, I. (2022) Cellulose-synthesizing
562 machinery in bacteria. *Cellulose* **29**, 2755-2777

563 6. Wong, H. C., Fear, A. L., Calhoon, R. D., Eichinger, G. H., Mayer, R., Amikam, D., Benziman,
564 M., Gelfand, D. H., Meade, J. H., Emerick, A. W., Bruner, R., Ben-Bassat, A., and Tal, R.
565 (1990) Genetic organization of the cellulose synthase operon in *Acetobacter xylinum*. *Proc.*
566 *Natl. Acad. Sci. U.S.A.* **87**, 8130-8134

567 7. Saxena, I. M., Kudlicka, K., Okuda, K., and Brown Jr, R. M. (1994) Characterization of
568 genes in the cellulose-synthesizing operon (acs operon) of *Acetobacter xylinum*:
569 Implications for cellulose crystallization. *J. Bacteriol.* **176**, 5735-5752

570 8. Standal, R., Iversen, T. G., Coucheron, D. H., Fjaervik, E., Blatny, J. M., and Valla, S. (1994)
571 A new gene required for cellulose production and a gene encoding cellulolytic activity in
572 Acetobacter xylinum are colocalized with the bcs operon. *J. Bacteriol.* **176**, 665-672
573 9. Kawano, S., Tajima, K., Kono, H., Erata, T., Munekata, M., and Takai, M. (2002) Effects of
574 endogenous endo-β-1,4-glucanase on cellulose biosynthesis in *Acetobacter xylinum*
575 ATCC23769. *J. Biosci. Bioeng.* **94**, 275-281
576 10. Tajima, K., Nakajima, K., Yamashita, H., Shiba, T., Munekata, M., and Takai, M. (2001)
577 Cloning and sequencing of the beta-glucosidase gene from *Acetobacter xylinum* ATCC
578 23769. *DNA Res.* **8**, 263-269
579 11. Tonouchi, N., Tahara, N., Kojima, Y., Nakai, T., Sakai, F., Hayashi, T., Tsuchida, T., and
580 Yoshinaga, F. (1997) A beta-glucosidase gene downstream of the cellulose synthase operon
581 in cellulose-producing acetobacter. *Biosci. Biotechnol. Biochem.* **61**, 1789-1790
582 12. McNamara, J. T., Morgan, J. L. W., and Zimmer, J. (2015) A Molecular Description of
583 Cellulose Biosynthesis. *Annu. Rev. Biochem.* **84**, 895-921
584 13. Kumagai, A., Mizuno, M., Kato, N., Nozaki, K., Togawa, E., Yamanaka, S., Okuda, K.,
585 Saxena, I. M., and Amano, Y. (2011) Ultrafine Cellulose Fibers Produced by *Asaia*
586 *bogorensis*, an Acetic Acid Bacterium. *Biomacromolecules* **12**, 2815-2821
587 14. Penttilä, P. A., Imai, T., Capron, M., Mizuno, M., Amano, Y., Schweins, R., and Sugiyama,
588 J. (2018) Multimethod approach to understand the assembly of cellulose fibrils in the

589 biosynthesis of bacterial cellulose. *Cellulose*

590 15. Hu, S. Q., Gao, Y. G., Tajima, K., Sunagawa, N., Zhou, Y., Kawano, S., Fujiwara, T., Yoda,
591 T., Shimura, D., Satoh, Y., Munekata, M., Tanaka, I., and Yao, M. (2010) Structure of
592 bacterial cellulose synthase subunit D octamer with four inner passageways. *Proc. Natl.*
593 *Acad. Sci. U.S.A.* **107**, 17957-17961

594 16. Sunagawa, N., Fujiwara, T., Yoda, T., Kawano, S., Satoh, Y., Yao, M., Tajima, K., and Dairi,
595 T. (2013) Cellulose complementing factor (Ccp) is a new member of the cellulose synthase
596 complex (terminal complex) in Acetobacter xylinum. *J. Biosci. Bioeng.* **115**, 607-612

597 17. Omadjela, O., Narahari, A., Strumillo, J., Melida, H., Mazur, O., Bulone, V., and Zimmer, J.
598 (2013) BcsA and BcsB form the catalytically active core of bacterial cellulose synthase
599 sufficient for in vitro cellulose synthesis. *Proc. Natl. Acad. Sci. U.S.A.***110**, 17856-17861

600 18. Imai, T., Sun, S.-j., Horikawa, Y., Wada, M., and Sugiyama, J. (2014) Functional
601 reconstitution of cellulose synthase in *Escherichia coli*. *Biomacromolecules* **15**, 4206–4213

602 19. Du, J., Vepachedu, V., Cho, S. H., Kumar, M., and Nixon, B. T. (2016) Structure of the
603 cellulose synthase complex of *Gluconacetobacter hansenii* at 23.4 A resolution. *PLoS ONE*
604 **11**, e0155886

605 20. Sun, S.-j., Imai, T., Sugiyama, J., and Kimura, S. (2017) CesA protein is included in the
606 terminal complex of Acetobacter. *Cellulose* **24**, 2017–2027

607 21. Sun, S.-j., Horikawa, Y., Wada, M., Sugiyama, J., and Imai, T. (2016) Site-directed

608 mutagenesis of bacterial cellulose synthase highlights sulfur–arene interaction as key to
609 catalysis. *Carbohydr. Res.* **434**, 99–106
610 22. Acheson, J. F., Ho, R. Y., Goularte, N. F., Cegelski, L., and Zimmer, J. (2021) Molecular
611 organization of the *E. coli* cellulose synthase macrocomplex. *Nat. Struct. Mol. Biol.* **28**, 310-
612 318
613 23. Santos, C. R., Paiva, J. H., Sforça, M. L., Neves, J. L., Navarro, R. Z., Cota, J., Akao, P. K.,
614 Hoffmam, Z. B., Meza, A. N., Smetana, J. H., Nogueira, M. L., Polikarpov, I., Xavier-Neto,
615 J., Squina, F. M., Ward, R. J., Ruller, R., Zeri, A. C., and Murakami, M. T. (2012) Dissecting
616 structure-function-stability relationships of a thermostable GH5-CBM3 cellulase from
617 *Bacillus subtilis* 168. *Biochem. J.* **441**, 95-104
618 24. Acheson, J. F., Derewenda, Z. S., and Zimmer, J. (2019) Architecture of the Cellulose
619 Synthase Outer Membrane Channel and Its Association with the Periplasmic TPR Domain.
620 *Structure* **27**, 1855-1861.e3
621 25. Nojima, S., Fujishima, A., Kato, K., Ohuchi, K., Shimizu, N., Yonezawa, K., Tajima, K., and
622 Yao, M. (2017) Crystal structure of the flexible tandem repeat domain of bacterial cellulose
623 synthesis subunit. *Sci. Rep.* **7**, 13018
624 26. Perez-Riba, A., and Itzhaki, L. S. (2019) The tetratricopeptide-repeat motif is a versatile
625 platform that enables diverse modes of molecular recognition. *Curr. Opin. Struct. Biol.* **54**,
626 43-49

627 27. Abidi, W., Zouhir, S., Caleechurn, M., Roche, S., and Krasteva, P. V. (2021) Architecture and
628 regulation of an enterobacterial cellulose secretion system. *Sci. Adv.* **7**, eabd8049
629 28. Uto, T., Ikeda, Y., Sunagawa, N., Tajima, K., Yao, M., and Yui, T. (2021) Molecular Dynamics
630 Simulation of Cellulose Synthase Subunit D Octamer with Cellulose Chains from Acetic
631 Acid Bacteria: Insight into Dynamic Behaviors and Thermodynamics on Substrate
632 Recognition. *J.Chem.Theory Comput.* **17**, 488-496
633 29. Toyosaki, H., Naritomi, T., Seto, A., Matsuoka, M., Tsuchida, T., and Yoshinaga, F. (1995)
634 Screening of Bacterial Cellulose-producing Acetobacter Strains Suitable for Agitated
635 Culture. *Biosci. Biotechnol. Biochem.* **59**, 1498-1502
636 30. Nakai, T., Moriya, A., Tonouchi, N., Tsuchida, T., Yoshinaga, F., Horinouchi, S., Sone, Y.,
637 Mori, H., Sakai, F., and Hayashi, T. (1998) Control of expression by the cellulose synthase
638 (bcsA) promoter region from *Acetobacter xylinum* BPR 2001. *Gene* **213**, 93-100
639 31. Rao, F., Pasunooti, S., Ng, Y., Zhuo, W., Lim, L., Liu, A. W., and Liang, Z. X. (2009)
640 Enzymatic synthesis of c-di-GMP using a thermophilic diguanylate cyclase. *Anal. Biochem.*
641 **389**, 138-142
642 32. Crameri, A., Whitehorn, E. A., Tate, E., and Stemmer, W. P. C. (1996) Improved green
643 fluorescent protein by molecular evolution using DNA shuffling. *Nat. Biotechnol.* **14**, 315-
644 319
645 33. https://www.gene.mie-u.ac.jp/Protocol/Original/Transform-Comp-Cell-Freeze.html, the

646 latest access date: April 7 2022

647 34. Updegraff, D. M. (1969) Semimicro determination of cellulose inbiological materials. *Anal.*

648 *Biochem.* **32**, 420-424

649 35. Stahlberg, J., Johansson, G., and Pettersson, G. (1993) *Trichoderma reesei* has no true exo-

650 cellulase: All intact and truncated cellulase produce new reducing end groups on cellulose.

651 *Biochim. Biophys. Acta - Gen. Subj.* **1157**, 107-113

652 36. Studier, F. W. (2005) Protein production by auto-induction in high density shaking cultures.

653 *Protein Expr. Purif.* **41**, 207-234

654 37. Hashimoto, A., Shimono, K., Horikawa, Y., Ichikawa, T., Wada, M., Imai, T., and Sugiyama,

655 J. (2011) Extraction of cellulose-synthesizing activity of *Gluconacetobacter xylinus* by

656 alkylmaltoside. *Carbohydr. Res.* **346**, 2760–2768

657

658 **Abbreviations**

659 The abbreviations used are: Bcs, bacterial cellulose synthase; CD, catalytic domain; c.v., column

660 volume; c-di-GMP, cyclic-di-guanosine monophosphate; DDM, *n*-β-D-maltopyranoside; DGC,

661 diguanylate cyclase; DP, degree of polymerization;. FL, full length; GH, glycoside hydrolase; IMAC,

662 immobilized metal affinity chromatography; PASC, phosphoric acid swollen cellulose; TBS, tris-

663 buffered saline; TBS-T, tris-buffered saline with Tween-20; TPR, tetratricopeptide repeat

664

665 **Figure legends**

666 **Figure 1. Deletion of the *E. coli* endogenous *bcsA* gene**

667 **A** Schematic diagram of the experiment for deleting the endogenous *bcsA* gene using the Red/ET

668 recombination system. The primer sequences used are listed in Table S1. **B** Electrophoresis pattern of colony-

669 direct PCR using two pairs of primers. M: Molecular weight marker (Marker 6 (Nippon Gene Co. Ltd., Tokyo,

670 Japan)); Δ*bcsA*: *bcsA*-deleted BL21; WT: wild-type BL21. **C** Quantification of endogenous cellulose

671 synthesis in BL21-GM and BL21 cells. The CESEC system (18), which uses DGC expression to synthesize

672 c-di-GMP to activate bacterial cellulose synthase, was used to count the amount of cellulose that used DGC

673 expression (bottom). The expression of DGC was confirmed by WB using an anti-Trx antibody (top). The

674 experiments were performed in triplicate (n = 3) and are represented as mean ± standard error of the mean

675 (SEM), together with each of the data values. Statistical tests (Student's t-test) were performed using the

676 built-in function in Microsoft Excel (TTEST).

677

678

679 **Figure 2. *in vivo* cellulose-synthesizing activity of recombinant Bcs-complex**

680 **A** Cellulose-synthesizing activity of the recombinant Bcs-complexes tested in this study: the amount of

681 cellulose synthesized by the CESEC system (18) with BL21-GM (Δ*bcsA*) is shown for each recombinant

682 protein. All experiments were performed in triplicate (n = 3) and are represented as mean ± SEM together

683 with the significance of difference: * for $p < 0.05$, ** for $p < 0.01$, *** for $p < 0.001$, and *n.s.* for not significant

684 ($p > 0.1$) as a result of Student's t-test, which was performed using the built-in function of Microsoft Excel

685 (TTEST). **B** Western blotting (WB) was performed for the CESEC experiment to check the expression of

686 BcsA, BcsB, BcsC, BcsD, and $_{TRX}$DGC. Cultures with and without DGC expression were tested. For BcsA,

687 the data are shown separately for the oligomer and monomer bands. Due to the limited number of wells in

688 the SDS-PAGE gel, the gel was divided into two parts for electrophoresis.

689

690

691

692 **Figure 3. Purification of $BcsABCD_{H6}$**

693 **A** Western blotting (WB) analysis of the purification process: M, membrane fraction; S, solubilized fraction;

694 F, IMAC unbound fraction; E, IMAC-eluted fraction. Three protein samples, wild-type ($BcsABCD_{H6}$),

695 D333N on BcsA ($BcsA^{D333N}BCD_{H6}$), and W373A on BcsA ($BcsA^{W373A}BCD_{H6}$), were analyzed using the

696 antibodies indicated. **B** WB analyses of the eluate from three independent purification experiments for each

697 of the three protein samples.

698 Approximately 2 μg of the protein was loaded onto the gel for WB with BcsA, BcsB, and BcsC antibodies,

699 and 1 μg of the protein was added to the gel for WB with BcsD antibody. For BcsA, the data are shown

700 separately for the oligomer and monomer bands.

701

702

703 **Figure 4. Effect of cellulase treatment to the purification of Bcs-complex**

704 **A**, Western blot images of IMAC-eluted fractions of $BcsABCD_{H6}$ after treatment with wild-type cellulase

705 (BsCel5A_FL and BsCel5A_CD). Coomassie Brilliant Blue (CBB)-stained images were used as loading

706 controls. **B** Band intensity in western blot analysis of **A**. Error bars indicate SEM, and the significance of the

707 difference as a result of Student's *t*-test, which was performed using the built-in function of Microsoft Excel

708 (TTEST), is indicated by the symbols: ** for $p < 0.01$, *** for $p < 0.001$, and *n.s.* for not significant ($p >$

709 0.1). **C**, Western blot images of IMAC-eluted fractions of $BcsABCD_{H6}$ after cellulase mutant (BsCel5A_FLm

710 and BsCel5A_CDm) treatment. CBB-stained images were visualized using BcsD as a loading control. **D**,

711 Band intensity in western blot analysis of **C**. Error bars indicate SEM, and Student's *t*-test, which was

712 performed using the built-in function of Microsoft Excel (TTEST), showed no significant difference ($p >$

713 0.1; eight independent replicates).

714 For BcsA, the data are shown separately for the oligomer band, monomer band, and their sum. Each elution

715 sample (~0.2 mg/mL) was added to an SDS-PAGE gel in 10 μL (anti-BcsA and anti-BcsB) and 1 μL (anti-

716 BcsD and CBB stain), respectively. Elution samples for CBB staining were loaded into gel wells 10-fold

717 more than those for WB (BcsD lane).

718

719 **Figure 5. Effect of cellulase treatment on the purification of mutant Bcs-complex**

720 **A** Western blot images of IMAC-eluted fractions of $BcsABCD_{H6}$, $BcsA^{D333N}BCD_{H6}$, and $BcsA^{W373A}BCD_{H6}$.

721 CBB-stained images were visualized using BcsD as a loading control. **B** Band intensity in western blot

722 analysis of **A**. An error bar indicates SEM, and the significance of the difference as a result of Student's *t*-

723 test, which was performed using the built-in function of Microsoft Excel (TTEST), is indicated by the

724 symbols † for $p < 0.1$, ** for $p < 0.01$, *** for $p < 0.001$, and *n.s.* for not significant ($p > 0.1$). **C**, Western

725 blot images of IMAC-eluted fractions of $BcsA^{D333N}BCD_{H6}$ and $BcsA^{W373A}BCD_{H6}$ after treatment with wild-

726 type cellulase (BsCel5A_FL and BsCel5A_CD). **D** and **E** Band intensity on western blot analysis of **C**: D for

727 $BcsA^{D333N}BCD$ and E for $BcsA^{W373A}BCD$. An error bar indicates SEM, and the significance of the difference

728 as a result of Student's *t*-test, which was performed using the built-in function of Microsoft Excel (TTEST),

729 showed no significant difference between any dataset.

730 All experiments were performed with four independent replicates ($n = 4$). For BcsA, the data are shown

731 separately for the oligomer band, monomer band, and their sum. Each elution sample (~0.2 mg/mL) was

732 added to an SDS-PAGE gel in 10 μL (anti-BcsA and anti-BcsB) and 1 μL (anti-BcsD and CBB stain),

733 respectively. Elution samples for CBB staining were loaded into gel wells 10-fold more than those for WB

734 (BcsD lane).

735

736 **Figure 6. Pull-down assay with the Bcs subunits**

737 **A** Schematic diagram showing the partners (bait and prey proteins) in a pull-down assay for each subunit of

738 BcsABCD. Alphabets on the cartoon indicate panels B–D (the result of pull-down experiments), by which

739 the subunit-subunit interaction was surveyed. **B** Western blot images of the pull-down assay using $BcsD_{StrepII}$

740 (bait) with crude BcsAB (prey). The pull-down fraction was analyzed by western blot using anti-BcsA, anti-

741 BcsB, and anti-Streptag antibodies. **C** Western blot images of the pull-down assay using $BcsD_{StrepII}$ (bait)

742 with purified $_{H6}BcsC_TPR_{H6}$ (prey). The pull-down fraction was analyzed by CBB staining and western

743 blotting using anti-His5 and anti-Streptag antibodies. **D** Western blot images of the pull-down assay using

744 $_{H6}BcsC_TPR_{H6}$ (bait) with crude BcsAB (prey). The pull-down fraction was analyzed by western blot using

745 anti-BcsA, anti-BcsB, and anti-His5 antibodies. **E** Western blot images of the pull-down assay using

746 $BcsD_{StrepII}$ (bait) with crude BcsAB (prey_1) and purified $_{H6}BcsC_TPR_{H6}$ (prey_2). The pull-down fraction

747 was analyzed by western blot using anti-BcsA, anti-BcsB, anti-His5, and anti-Streptag antibodies. Input:

748 sample immediately after mixing; pull-down: elution fraction after pull-down. All the detailed methods are

749 described in the “Experimental Procedures” section of the text.

750

751

752 **Figure 7. The hypothetical two-state model for the type I Bcs-complex**

753 Hypothetical two-state model for the Bcs-complex: basal state (left) and active state (right). In this model,
754 BcsD plays a key role in the periplasmic space to control the state of the complex separately from the state
755 of the BcsA enzyme (1,2). In the active state (right), BcsD draws the glucan chains in its octameric ring and
756 brings those chains to the channel pore of BcsC in the outer membrane like a "button whirligig'. The TPR
757 domain in BcsC may escort the BcsD protein to correctly transfer the glucan chains in BcsD to the BcsC
758 channel. In the basal state (left), BcsD docks with the BcsB complex given that BcsB is located in the
759 periplasmic space (1) as well as BcsD (12,20). In the model, BcsD in the basal state also docks with BcsC
760 without interfering with BcsB and is ready to draw the glucan chains in it once BcsAB starts synthesizing
761 and extruding out the glucan chain. Thus, BcsD in this state may be a standby state for effectively transferring
762 glucan chains into the extracellular space through the BcsC channel once BcsA is activated. Subunits that
763 were not assessed in this study are indicated in gray.

764

765 Table 1. Experimental resources to express the proteins in this study

766

Material	Source	Description	Reference
		Bacterial cellulose synthase	
pQE-BcsAB (GOI* was inserted between EcoRI and KpnI site in pQE-80L vector (Qiagen Inc.))	LC428282 (*Komagataeibacter sucrofermentans* JCM9730)	Expression vector for BcsAB protein without tags	Imai et al. 2014
pQE-BcsA^{D333N}B (GOI* was inserted between EcoRI and KpnI site in pQE-80L vector (Qiagen Inc.))	LC428282 (*Komagataeibacter sucrofermentans* JCM9730)	Expression vector for BcsAB protein with a catalytic-deficient point mutation of D333N, without tags	Sun et al., 2016
pQE-BcsA^{W373A}B (GOI* was inserted between EcoRI and KpnI site in pQE-80L vector (Qiagen Inc.))	LC428282 (*Komagataeibacter sucrofermentans* JCM9730)	Expression vector for BcsAB protein with a catalytic-deficient point mutation of W373A, without tags	Sun et al., 2016
pQE-BcsABCD (GOI was inserted between EcoRI and HindIII site in pQE-80L vector (Qiagen Inc.))	LC687564 (*Komagataeibacter sucrofermentans* JCM9730)	Expression vector for BcsABCD complex without tags	This study
pQE-BcsABCD$_{H6}$ (GOI was inserted between EcoRI and HindIII site in pQE-80L vector (Qiagen Inc.))	LC687564 (*Komagataeibacter sucrofermentans* JCM9730)	Expression vector for BcsABCD complex with hexahistidine-tag at the C-terminal of BcsD protein	This study
pQE-BcsABC$_{H6}$D (GOI was inserted between EcoRI and HindIII site in pQE-80L vector (Qiagen Inc.))	LC687564 (*Komagataeibacter sucrofermentans* JCM9730)	Expression vector for BcsABCD complex with hexahistidine-tag at the N-terminal of BcsD protein	This study
pQE-BcsABCD$_{GFPuvH6}$ (GOI was inserted between EcoRI and HindIII site in	LC687564 (*Komagataeibacter sucrofermentans*	Expression vector for BcsABCD complex with GFPuv followed by hexahistidine-tag at the C-terminal	This study

pQE-80L vector (Qiagen Inc.))	JCM9730)	of BcsD protein	
pQE-BcsA^{D333N}BCD$_{H6}$ (GOI was inserted between EcoRI and HindIII site in pQE-80L vector (Qiagen Inc.))	LC687564 (*Komagataeibacter sucrofermentans* JCM9730)	Expression vector for BcsABCD complex with a catalytic-deficient point mutation of D333N introduced in BcsA; hexahistidine-tag is fused to the C-terminal of BcsD protein	This study
pQE-BcsA^{W373A}BCD$_{H6}$ (GOI was inserted between EcoRI and HindIII site in pQE-80L vector (Qiagen Inc.))	LC687564 (*Komagataeibacter sucrofermentans* JCM9730)	Expression vector for BcsABCD complex with a catalytic-deficient point mutation of W373A introduced in BcsA; hexahistidine-tag is fused to the C-terminal of BcsD protein	This study
pET-$_{H6}$BcsC_TPR$_{H6}$ (GOI was inserted between NdeI and XhoI site in pET28b (Novagene Inc.))	LC687564 (*Komagataeibacter sucrofermentans* JCM9730)	Expression vector for TPR domain of BcsC protein (Cys18 – Gly848): hexahistidine-tag is fused to both N- and C-terminal of the protein	This study
pET-BcsD$_{StrepII}$ (GOI was inserted between NcoI and HindIII site in pET28b vector (Novagen Inc.))	LC687564 (*Komagataeibacter sucrofermentans* JCM9730)	Expression vector for BcsD protein: Streptag(II) is fused to the C-terminal of BcsD protein	This study
Diguanylate cyclase (DGC)			
pBAD33et32-tDGC (Self-made vector in the previous study)	NP_229585 (*Thermotoga maritima* MSB8)	Expression vector of diguanylate cyclase with N-terminal truncation (K82 – S248) and a point mutation (R158A mutation): thioredoxin was fused to Nterminal end of the protein	This study
Cellulase			
pGEX-BsCel5A_FL (GOI was inserted between BamHI and XhoI site in	Z29076 (*Bacillus subtilis* strain 168)	Expression vector for full-length endoglucanase protein from *Bacillus subtilis* (BsCel5A):	This study

pGEX4T-3 (GE Healthcare Inc.))		signal-peptide sequence (from Met1 to Ala28) was removed; GST-tag is fused to the N-terminal of BsCel5A protein, which consists of glycosylhydrolase 5 domain (GH-5 domain, Ala29 – Thr332) and carbohydrate-binding module (CBM-3, Ile354 – Asn499)	
pGEX-BsCel5A_CD (GOI was inserted between BamHI and XhoI site in pGEX4T-3 (GE Healthcare Inc.))	Z29076 (*Bacillus subtilis* strain 168)	Expression vector for catalytic domain (A29 – T332) of BsCel5A: GST-tag is fused to the N-terminal of the protein, which lacks the signal peptide sequence (Met1 – Ala28)	This study
pGEX-BsCel5A_FL^{m} (GOI was inserted between BamHI and XhoI site in pGEX4T-3 (GE Healthcare Inc.))	Z29076 (*Bacillus subtilis* strain 168)	Expression vector for full-length BsCel5A with activity-deficient double mutation (E169Q/E257Q): GST-tag is fused to the N-terminal of the protein, which lacks the signal peptide sequence (Met1 – Ala28)	This study
pGEX-BsCel5A_CD^{m} (GOI was inserted between BamHI and XhoI site in pGEX4T-3 (GE Healthcare Inc.))	Z29076 (*Bacillus subtilis* strain 168)	Expression vector for catalytic domain (A29 – T332) of BsCel5A with activity-deficient double mutation (E169Q/E257Q): GST-tag is fused to the N-terminal of the protein, which lacks the signal peptide sequence (Met1 – Ala28)	This study

767

768 * GOI: gene of interest

769

Figure 1

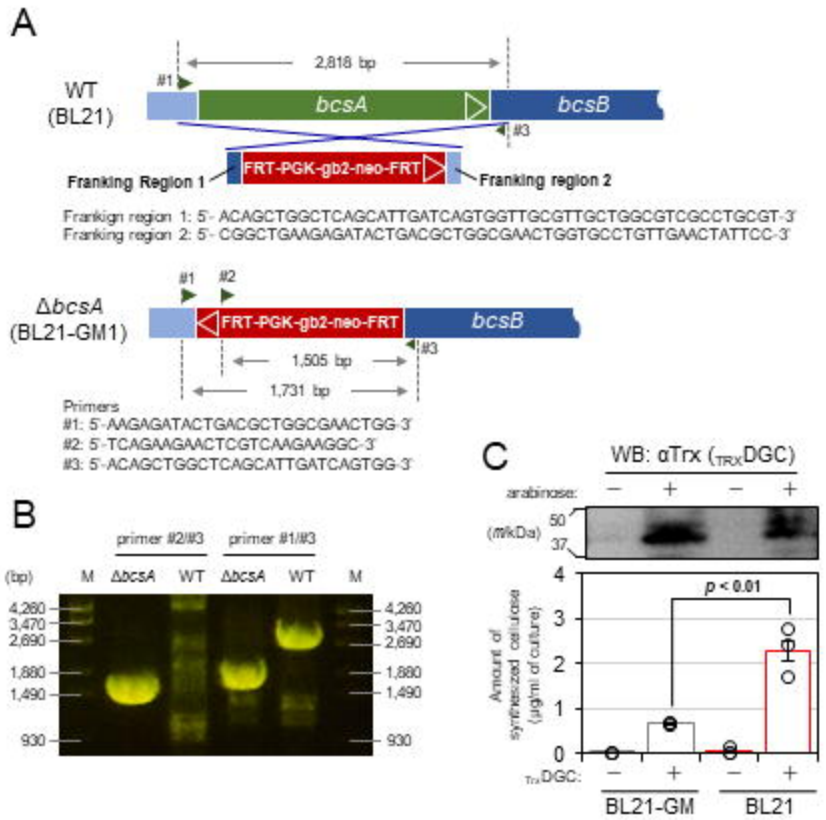
A
2,818 bp
WT
(BL21)
#1
bcsA
bcsB
#3
FRT-PGK-gb2-neo-FRT
Franking Region 1
Franking region 2
Frankign region 1: 5'- ACAGCTGGCTCAGCATTGATCAGTGGTTGCGTTGCTGGCGTCGCCTGCGT-3'
Franking region 2: 5'- CGGCTGAAGAGATACTGACGCTGGCGAACTGGTGCCTGTTGAACTATTCC-3'
ΔbcsA
(BL21-GM1)
#1
#2
FRT-PGK-gb2-neo-FRT
bcsB
#3
1,505 bp
1,731 bp
Primers
#1: 5'-AAGAGATACTGACGCTGGCGAACTGG-3'
#2: 5'-TCAGAAGAACTCGTCAAGAAGGC-3'
#3: 5'-ACAGCTGGCTCAGCATTGATCAGTGG-3'
B
primer #2/#3
primer #1/#3
(bp)
M
ΔbcsA
WT
ΔbcsA
WT
M
4,260
3,470
2,690
1,880
1,490
930
C
WB: αTrx (TRXDGC)
arabinose:
−
+
−
+
(mkDa)
50
37
Amount of synthesized cellulose (μg/ml of culture)
p < 0.01
4
3
2
1
0
TrxDGC:
−
+
−
+
BL21-GM
BL21

Figure 2

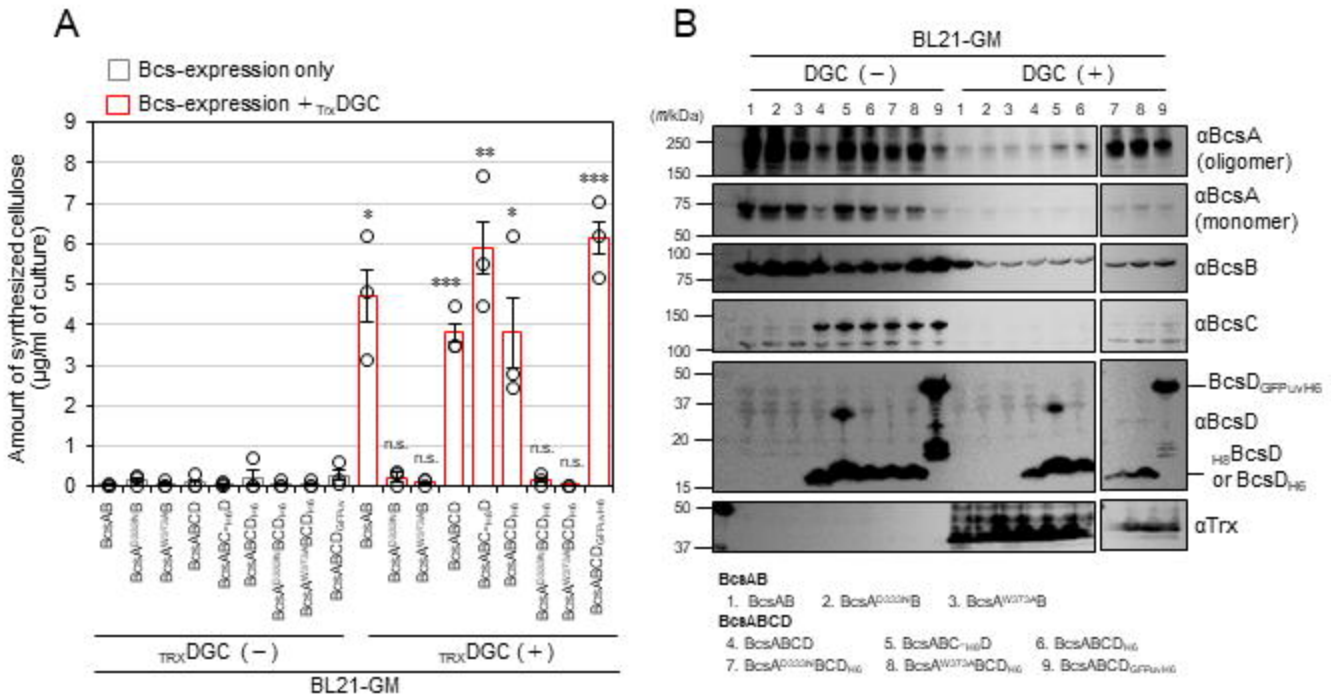
A
Bcs-expression only
Bcs-expression + TrxDGC
Amount of synthesized cellulose (μg/ml of culture)
n.s.
TRXDGC (−)
TRXDGC (+)
BL21-GM
B
BL21-GM
DGC (−)
DGC (+)
(mkDa)
αBcsA (oligomer)
αBcsA (monomer)
αBcsB
αBcsC
BcsDGFPuvH6
αBcsD
H8BcsD or BcsDH6
αTrx
BcsAB
1. BcsAB 2. BcsAD320NB 3. BcsAW373AB
BcsABCD
4. BcsABCD 5. BcsABC−H6D 6. BcsABCDH6
7. BcsAD320NBCDH6 8. BcsAW373ABCDH6 9. BcsABCDGFPuvH6

Figure 3

A

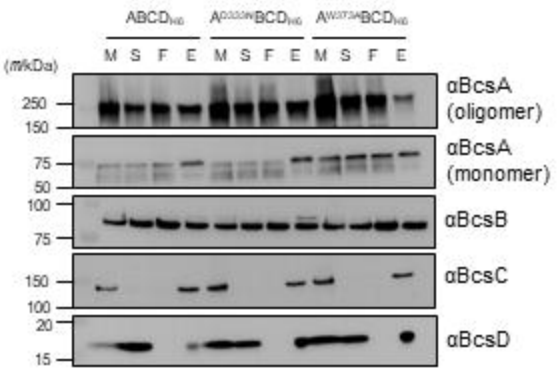
ABCD$_{H6}$
A^{D333N}BCD$_{H6}$
A^{W373A}BCD$_{H6}$
M S F E M S F E M S F E
(m/kDa)
250
150
75
50
100
75
150
100
20
15
αBcsA (oligomer)
αBcsA (monomer)
αBcsB
αBcsC
αBcsD

B

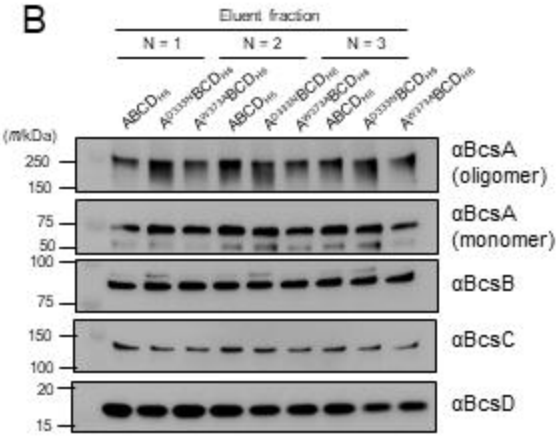
Eluent fraction
N = 1
N = 2
N = 3
ABCD$_{H6}$
A^{D333N}BCD$_{H6}$
A^{W373A}BCD$_{H6}$
ABCD$_{H6}$
A^{D333N}BCD$_{H6}$
A^{W373A}BCD$_{H6}$
ABCD$_{H6}$
A^{D333N}BCD$_{H6}$
A^{W373A}BCD$_{H6}$
(m/kDa)
250
150
75
50
100
75
150
100
20
15
αBcsA (oligomer)
αBcsA (monomer)
αBcsB
αBcsC
αBcsD

Figure 4

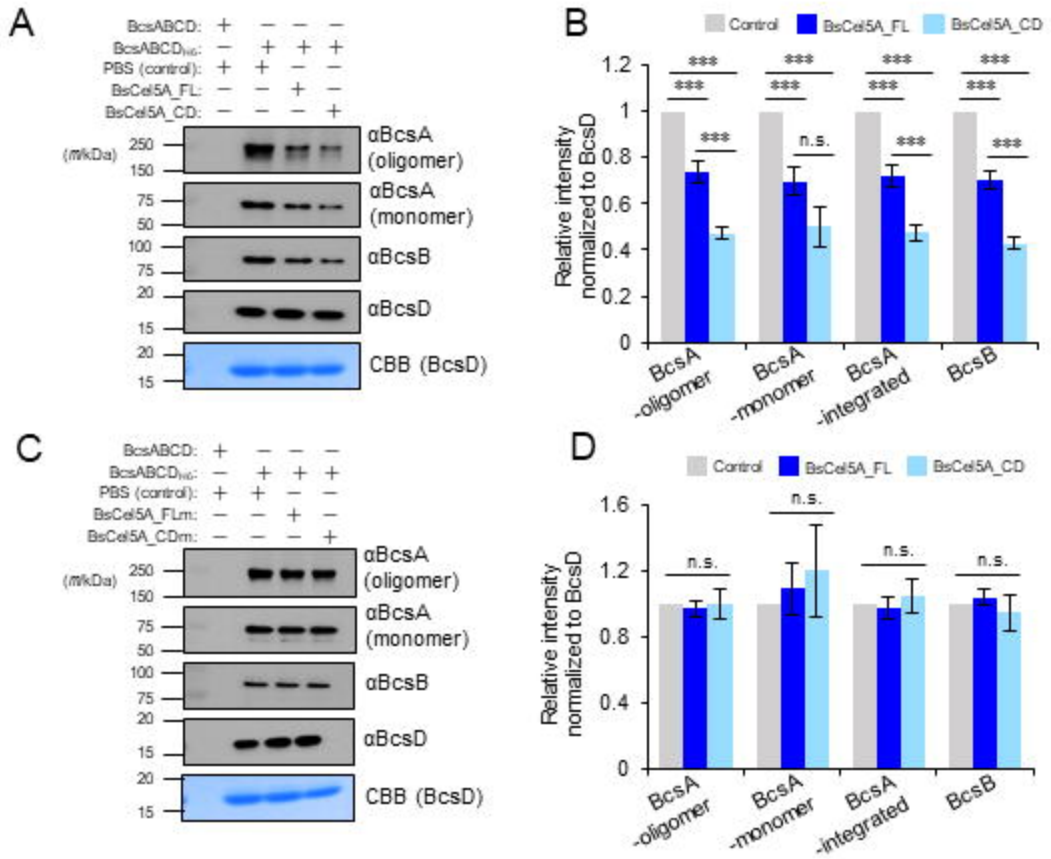
A
BcsABCD:
BcsABCD$_{his}$:
PBS (control):
BsCel5A_FL:
BsCel5A_CD:
(mkDa)
αBcsA (oligomer)
αBcsA (monomer)
αBcsB
αBcsD
CBB (BcsD)
B
Control
BsCel5A_FL
BsCel5A_CD
Relative intensity normalized to BcsD
BcsA -oligomer
BcsA -monomer
BcsA -integrated
BcsB
n.s.
C
BsCel5A_FLm:
BsCel5A_CDm:
D

Figure 5

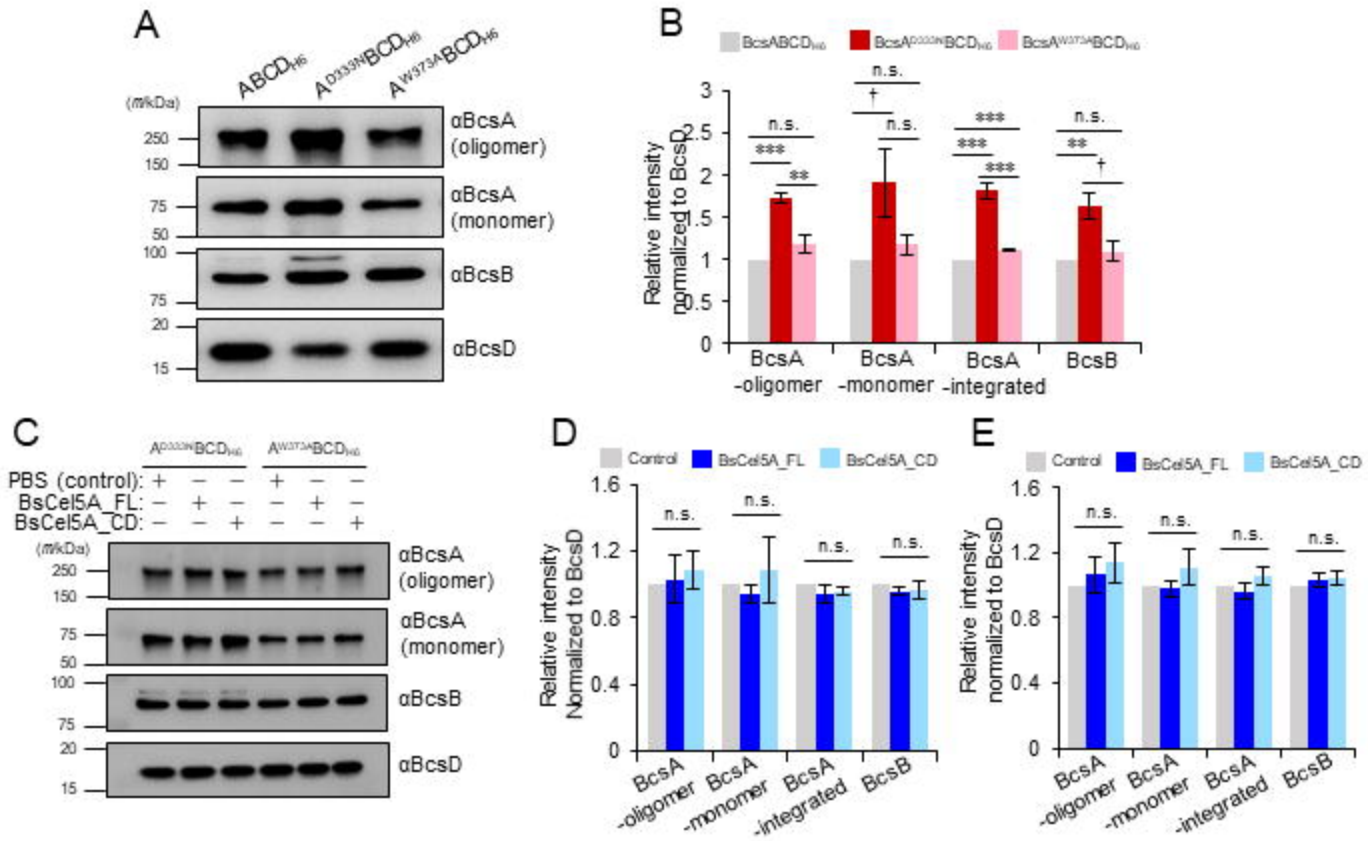
A
ABCD$_{H6}$
A^{D333N}BCD$_{H6}$
A^{W373A}BCD$_{H6}$
(mkDa)
250
150
75
50
100
75
20
15
αBcsA (oligomer)
αBcsA (monomer)
αBcsB
αBcsD
B
BcsABCD$_{H6}$
BcsA^{D333N}BCD$_{H6}$
BcsA^{W373A}BCD$_{H6}$
Relative intensity normalized to BcsD
BcsA -oligomer
BcsA -monomer
BcsA -integrated
BcsB
n.s.
***
**
†
C
A^{D333N}BCD$_{H6}$
A^{W373A}BCD$_{H6}$
PBS (control):
BsCel5A_FL:
BsCel5A_CD:
(mkDa)
250
150
75
50
100
75
20
15
αBcsA (oligomer)
αBcsA (monomer)
αBcsB
αBcsD
D
Control
BsCel5A_FL
BsCel5A_CD
Relative intensity Normalized to BcsD
BcsA -oligomer
BcsA -monomer
BcsA -integrated
BcsB
n.s.
E
Control
BsCel5A_FL
BsCel5A_CD
Relative intensity normalized to BcsD
BcsA -oligomer
BcsA -monomer
BcsA -integrated
BcsB
n.s.

Figure 6

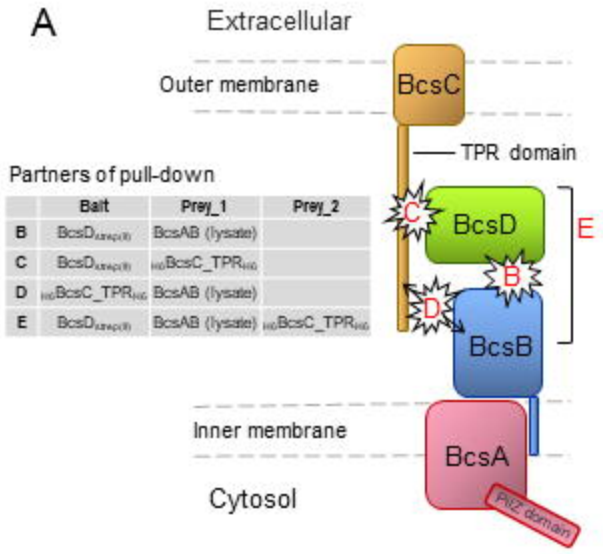

Partners of pull-down

	Bait	Prey_1	Prey_2
B	$BcsD_{strep(II)}$	BcsAB (lysate)	
C	$BcsD_{strep(II)}$	$_{H6}BcsC_TPR_{H6}$	
D	$_{H6}BcsC_TPR_{H6}$	BcsAB (lysate)	
E	$BcsD_{strep(II)}$	BcsAB (lysate)	$_{H6}BcsC_TPR_{H6}$

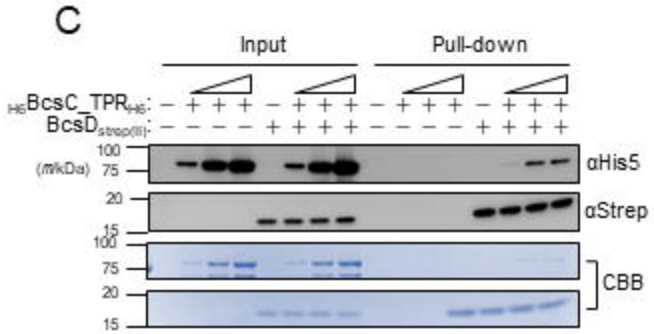

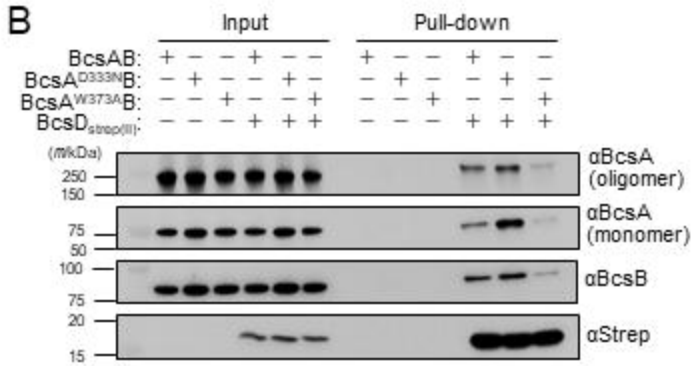

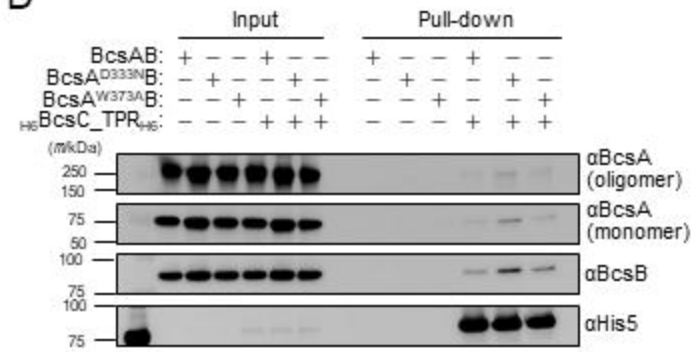

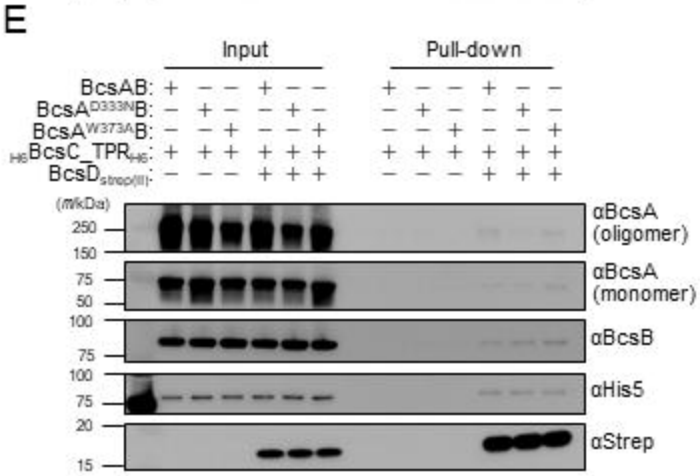

Figure 7

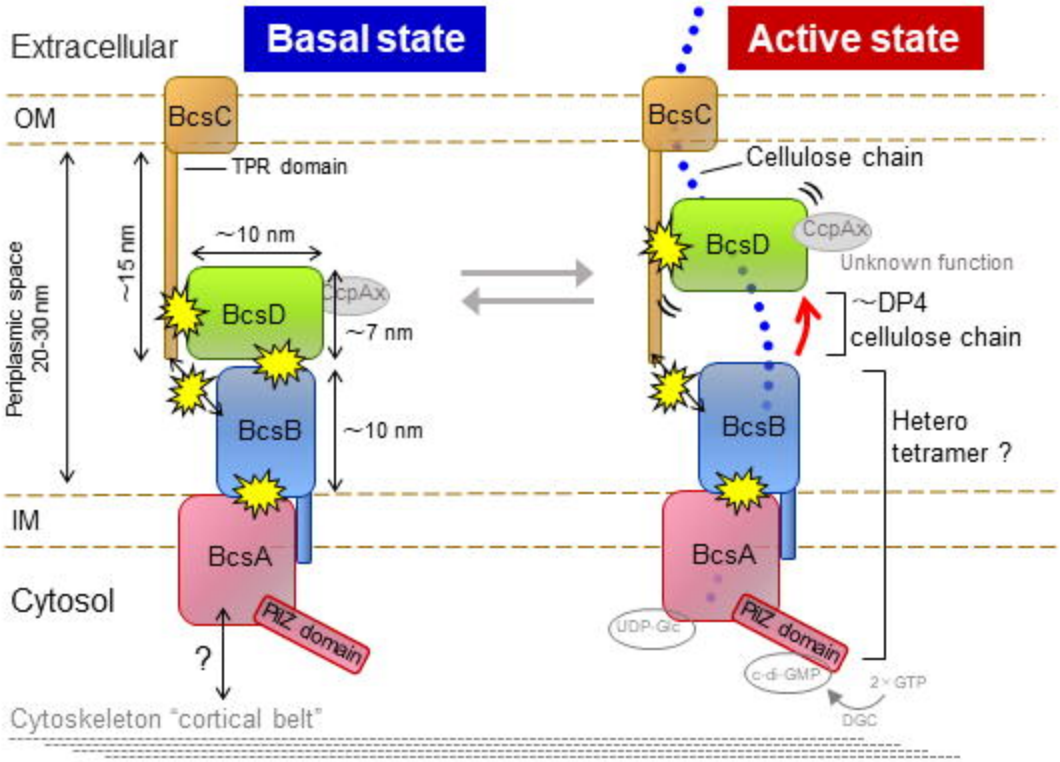
Extracellular
Basal state
Active state
OM
BcsC
TPR domain
Periplasmic space
20-30 nm
~15 nm
~10 nm
BcsD
CcpAx
~7 nm
BcsB
~10 nm
IM
BcsA
Cytosol
PilZ domain
?
Cytoskeleton "cortical belt"
BcsC
Cellulose chain
BcsD
CcpAx
Unknown function
~DP4
cellulose chain
BcsB
Hetero
tetramer ?
BcsA
UDP-Glc
PilZ domain
c-di-GMP
2 × GTP
DGC